Astronomy & Astrophysics manuscript no.
(will be inserted by hand later)

Radial $B-V/V-K$ color gradients, extinction-free $Q_{\rm BVK}$ combined color indices, and the history of star formation of the Cartwheel ring galaxy

E.I. Vorobyov[1] and D. Bizyaev[2]

[1] Institute of Physics, Stachki 194, Rostov-on-Don, Russia
e-mail: eduard_vorobev@mail.ru
[2] Sternberg Astronomical Institute, Universitetskiy prospect 13, Moscow, Russia
e-mail: dmbiz@sai.msu.ru

Abstract. In this paper we model and analyse the $B-V/V-K$ radial color gradients observed in the Cartwheel ring galaxy. Along with the color-color diagrams, we use the $Q_{\rm BVK}$ combined color indices, which minimise the uncertainties in the observed $B-V$ and $V-K$ colors introduced by dust extinction. To model the optical and near-infrared color properties of the Cartwheel galaxy, we assume that an intruder galaxy generates an expanding ring density wave in the Cartwheel's disk, which in its turn triggers massive star formation along the wave's perimeter according to the Schmidt law. We use the population synthesis to calculate the color properties of stellar populations formed in the expanding density wave. The results of color modelling suggest that the pre-collision Cartwheel was a late-type spiral, embedded in an extensive gaseous disk of sub-critical surface density. The properties of the old stellar disk are typical for the late-type Freeman disks, with the central surface brightness in V-band and the scale length being $\mu_{\rm V}^0 = 21.0$ mag arcsec^{-2} and $R_0 = 2$ kpc respectively. The pre-collision gaseous disk has a metallicity gradient ranging from $z = z_\odot/5$ at the outer regions to $z = z_\odot$ in the central regions. At present, the wave of star formation has passed the initial extent of the pre-collision, old stellar disk and is currently moving in the predominantly gaseous, low-metallicity disk at the radius of 16 kpc. Neither young stellar populations formed in an expanding density wave, nor their mixture with the old, pre-collision stellar populations can reproduce the $B-V$ and $V-K$ colors of the Cartwheel's nucleus+inner ring. We find that an additional 10-Myr-old burst of star formation in the nuclear regions, along with the visual extinction of $A_{\rm V} = 1^{\rm m}.3$, might be responsible for the peculiar colors of the Cartwheel's nucleus.

Key words. Galaxies: individual: The Cartwheel – Galaxies: stellar content – Galaxies: formation:

1. Introduction

Ring galaxies are believed to be the result of a head-on galaxy-galaxy collision. Such a near-central collision generates an expanding ring density wave in the disk of a larger galaxy. It is likely that star formation will be induced along the wave's perimeter when the gas density exceeds a threshold (Appleton & Struck-Marcell 1987). As such a wave of star formation advances radially from the nucleus, it leaves behind evolved stellar populations, with the youngest stars located at the current position of the wave. It is expected that this might result in the radial color distribution of stars in the galactic disk, with the inner regions being redder than the outer parts of the disk. Indeed, observations of the Cartwheel ring galaxy (Marcum et al. 1992) reveal the presence of the optical and near-infrared $B-V/V-K$ radial color gradients in the galactic disk. Recent observations of a sample of northern ring galaxies by Appleton & Marston (1997) show that most of them exhibit radial color gradients similar to the pattern observed in the Cartwheel.

Numerical modelling of the Cartwheel's radial color gradients by Korchagin et al. (2001) shows that the young stellar populations formed in the expanding density wave exhibit regular reddening of colors towards the nucleus only for the sub-solar metallicities of the star-forming gas ($z \le z_\odot/2.5$). Even in the most favorable case of $z = z_\odot/5$, the model colors are much bluer as compared to those observed in the Cartwheel. Korchagin et al. (2001) argue that the pre-collision disk of old stars is needed to reconcile the model and the Cartwheel's colors. However, their conclusions are based on the direct quantitative comparison of the model and the Cartwheel's $B-V$ and $V-K$ colors, which is complicated due to uncertainties in the amount of internal extinction in the Cartwheel's disk.

Send offprint requests to: E.I. Vorobyov

In this paper we re-address the question of theoretical modelling of the $B-V/V-K$ radial color gradients observed in the Cartwheel galaxy. We attempt to exclude the complicated influence of dust extinction on the theoretical interpretation of the Cartwheel's $B-V/V-K$ radial color gradients. To do this, we use insensitive to dust extinction $Q_{\rm BVK}$ combined color indices. Such color indices were successfully applied for structure modelling of dusty galaxies by Zasov & Moiseev (1998) and Bizyaev et al. (2000, 2001).

In Sect. 2 we analyse the $Q_{\rm BVK}$ radial distribution observed in the Cartwheel's disk and consider the factors defining the value of $Q_{\rm BVK}$. In Sect. 3 we formulate the adopted model of star formation in the Cartwheel galaxy. In Sect. 4 we compare the model B-V/V-K radial color gradients and $Q_{\rm BVK}$ index profiles, obtained in the framework of a first major episode of star formation in the Cartwheel's disk, with the observed radial profiles. We consider a possibility that the Cartwheel has an old stellar disk typical for the late-type spirals. In Sect. 5 we attempt to model the peculiar colors of the Cartwheel's nucleus and the inner ring. The main results are summarized in Sect. 6.

2. Infrared and optical $B-V/V-K$ radial color gradients and $Q_{\rm BVK}$ combined color indices of the Cartwheel galaxy

The $B-V/V-K$ radial color gradients of the Cartwheel galaxy are shown in Fig. 1, which is a reproduction of Fig. 3 of Marcum et al. (1992). The annular points are numbered according to radius, beginning with the inner ring (point I) and ending with the outer ring (points VIII and IX). These colors have only been corrected for Galactic reddening using $A_{\rm B}=0^{\rm m}.22$ and the standard ISM extinction curve (Marcum et al. 1992).

Previous modelling of the Cartwheel's radial color gradient was seriously complicated by the uncertainties in the amount of internal extinction in the galactic disk. The internal extinction is only measured towards two bright HII regions in the Cartwheel's outer ring ($A_{\rm V}=1^m.94$) and is not applicable to the whole galactic disk. The value of internal extinction interior to the outer ring of $A_{\rm V}=0^{\rm m}.3$ has been estimated from the available HI + H_2 data (Korchagin et al. 2001). Clearly, correction for the internal extinction would greatly distort the observed Cartwheel's B-V/V-K radial color pattern, as shown by correction vectors in Fig. 1, and complicate the task of color interpretation.

To avoid the complicated influence of dust on the Cartwheel's radial color gradient, we use insensitive to dust extinction $Q_{\rm BVK}$ combined color index defined as:

$$Q_{\rm BVK}=(B-V)-\frac{E(B-V)}{E(V-K)}(V-K), \qquad (1)$$

where $(B-V)$ and $(V-K)$ are colors, and $E(B-V)$ and $E(V-K)$ are color excesses.

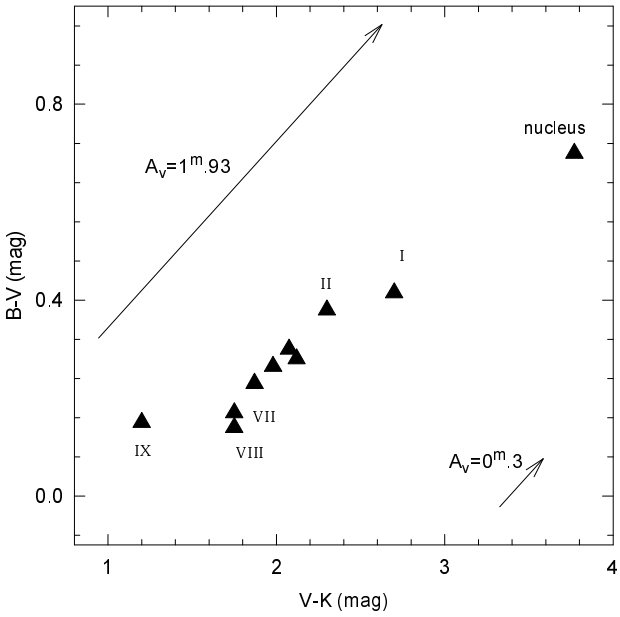

Fig. 1. Radial $B-V/V-K$ color gradients of the Cartwheel galaxy. This is a reproduction of Fig. 3 of Marcum et al. (1992).

For dust properties typical for the Galaxy ($R_{\rm V}=3.1$) the ratio of color excesses $E(B-V)/E(V-K)$ is equal to 0.365 (Cardelli et al. 1989). This value is valid for a "dust shield" approximation, i.e. when all dust is located between an observer and a galaxy. For a homogeneous mixture of dust and stars the ratio of color excesses $E(B-V)/E(V-K)$ is 10% less than for a "dust shield" approximation (Zasov & Moiseev 1998) and equal to 0.329. As to the Cartwheel galaxy, the internal extinction dominates at the outer ring and is comparable to the Galactic reddening in the inner part (Korchagin et al. 2001). Hence, we choose a "homogeneous mixture " approximation rather than a "dust shield" for modelling the Cartwheel's color properties.

The following factors define the value of $Q_{\rm BVK}$:

a) contribution of young, blue stars to the integrated flux, i.e. *the history of star formation in a certain region of a galaxy*. Figures 2a and 2b show the $Q_{\rm BVK}$ combined color indices of a single starburst superimposed on the old stellar population of 10 Gyr. Calculations are performed using the program of Worthey (1994). Metallicities of both the young and old stellar populations are equal to $z_\odot/5$ ([Fe/H]=-0.7). Figure 2a illustrates the influence of different relative contributions of young stars on the $Q_{\rm BVK}$ indices for a single 50-Myr-old starburst. Figure 2b shows the dependence of the $Q_{\rm BVK}$ indices on the age of a starburst. Here, both the young and old stellar populations contribute equally to the total stellar mass. As it can be

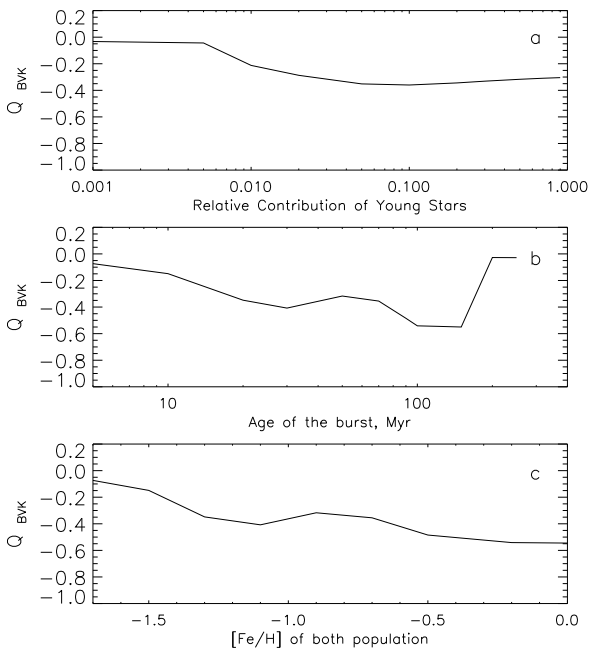

Fig. 2. The $Q_{\rm BVK}$ indices of a single starburst superimposed on the old stellar population of 10 Gyr. **a**) The influence of different relative contributions of young stars on the $Q_{\rm BVK}$ indices for a single starburst of 50 Myr old. **b**) Dependence of the $Q_{\rm BVK}$ indices on the age of a starburst. **c**) The $Q_{\rm BVK}$ indices as a function of metallicities of old and young stellar populations (equal for both populations).

seen, $Q_{\rm BVK}$ indices are sensitive to the age of a starburst and to the relative contribution of young stars.

Thus, a young burst of star formation should essentially influence the value of $Q_{\rm BVK}$. Relative increase of young stars in a certain region of a galaxy makes its colors bluer, thus, lowering the value of $Q_{\rm BVK}$ (Fig. 2a). On the other hand, the red supergiant flash (Charlot & Bruzual 1991) makes the luminosity of a young stellar cluster in the K-band to peak at 10 Myr after the burst, which noticeably lowers the value of $Q_{\rm BVK}$ (Fig. 2b).

b) *heavy element abundances.* Figure 2c gives $Q_{\rm BVK}$ indices as a function of metallicities of the old and young stellar populations (equal for both populations). The age of a single starburst is equal to 50 Myr. Metallicity gradient alone can essentially influence the value of $Q_{\rm BVK}$, while other starburst parameters remain unchanged.

c) *dust properties.* Cardelli et al. (1989) found that for the dust properties different from those of the Galaxy, i.e. for $R_{\rm V}$ other than 3.1, the ratio of color excesses $E(B-V)/E(V-K)$ changes. However, the Cartwheel's $Q_{\rm BVK}$ distribution remains qualitatively unchanged for a fairly wide range of $R_{\rm V}$. Thus, the value of $R_{\rm V} = 3.1$ is adopted for the rest of the paper.

Figure 3 shows the Cartwheel's $Q_{\rm BVK}$ distribution as a function of photometric annulus. Combined color indices are calculated using observational data of Marcum et al. (1992). The numbering of photometric annuli is in accordance with Fig. 3 of Marcum et al. (1992). The Cartwheel's $Q_{\rm BVK}$ radial distribution remarkably separates into three sub-profiles, which correspond to three structurally different parts of the Cartwheel: annuli 0 and 1 correspond to the nucleus and the inner ring, annuli 2-7 are the inter-ring region, and annuli 8 and 9 correspond to the outer ring. Combined color indices are insensitive to dust extinction and can be directly understood in terms of stellar populations. This natural separation of $Q_{\rm BVK}$ indices implies that the nucleus+inner ring, inter-ring region and the outer ring of the Cartwheel consist of different stellar populations.

Nucleus and the inner ring. The old stellar content of the nucleus is confirmed by the detection of late-type stellar absorption spectrum (Fosbury & Hawarden 1977). However, recent mid-infrared and Hα observations indicate that the old stellar populations may not totally dominate the spectrum. ISOCAM images (Charmandaris et al. 1999) show significant 7 μm and 15 μm emission in the nucleus and the inner ring, which implies a low-level star formation activity. Detection of weak Ha emission from the nucleus and inner ring also indicates that there might be some low-level star formation in the Cartwheel's central regions (Amram et al. 1998).

The inter-ring region. As Hα observations indicate, it is almost totally devoid of any star formation activity (Amram et al. 1998) and is probably populated by density wave born, post-collision stars with an admixture of old, pre-collision stars as implied by progressively reddened $B-V/V-K$ colors towards the Cartwheel's nucleus. The possibility that dust extinction is responsible for this reddening of colors will be tested in numerical simulations in Sect. 4.

The outer ring. Models of ring galaxy formation predict that the Cartwheel's outer ring is the current location of an outwardly propagating star formation wave (Appleton & Struck-Marcell 1987, Struck-Marcell & Appleton 1987). Hence, a large gradient in the $Q_{\rm BVK}$ distribution seen across the outer ring in Fig. 3 is indicative of rapid changes in the photometric properties of young stellar populations. Probably, the outer edge of the ring is so young that it has not yet produced any supergiants, whereas the inner edge is in the red-supergiant-flash stage (Marcum et al. 1992). Existence of the red supergiant flash is confirmed in observations of the young stellar cluster NGC 2004 in the LMC (Bica & Alloin 1987).

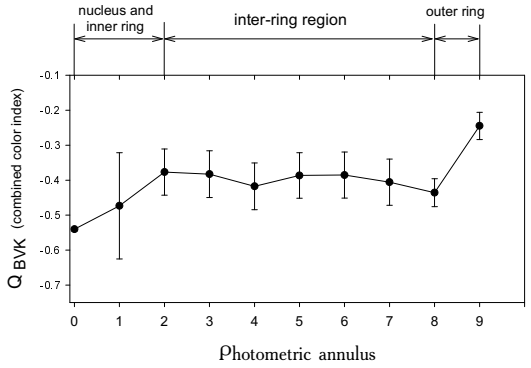

Fig. 3. The Cartwheel's $Q_{\rm BVK}$ distribution as a function of photometric annulus.

3. Theoretical modelling of the Cartwheel's color properties: orbit crowded density wave plus a Schmidt law of star formation

To model the optical and near-infrared color properties of the Cartwheel galaxy, we assume that the head-on galaxy-galaxy collision generates an outwardly propagating ring density wave in the disk of the Cartwheel. Additionally, we assume that the collision is central or near-central so that we can neglect the azimuthal variations in the strength of the density wave. Massive star formation in the Cartwheel galaxy is restricted to the outer ring, which is the current location of the density wave. Almost no sigh of star formation activity is found just behind and ahead of the outer ring (Higdon 1995).

To imitate the propagating star formation in the Cartwheel's disk, we assume that the star formation rate is proportional to a ring density enhancement expanding radially in a gaseous disk with velocity v. The density enhancement is given by a Gaussian function:

$$C(r-vt) = A(r)\ \exp\left[-\frac{(r-vt)^2}{L^2}\right], \qquad (2)$$

where $A(r)$ is the amplitude of the density enhancement and L is a half-width of the density enhancement. The balance of surface density of stars (Σ_s) at a distance r from the center and time t can be then written as follows (Korchagin et al. 2001):

$$\frac{d\Sigma_s}{dt} = -D + a\ C^n(r-vt), \qquad (3)$$

where the first term in the right-hand side of Eq. 3 is the rate of death of stars:

$$D = \frac{1}{\sum\limits_{m_1}^{m_2} m^{1-\alpha}}\ \sum_{m_1}^{m_2} m^{1-\alpha}\ a\ C^n(r-v(t-\tau_m)), \qquad (4)$$

where τ_m is the life-time of a star of mass m, and α is the slope of the IMF.

We consider a circular density enhancement propagating from the center of a gaseous disk to the present location of the Cartwheel's outer ring at 16 kpc (H_0 = 100 km s^{-1} Mpc^{-1}). The computational area is divided into 10 annuli as in Plate 1 of Marcum et al. (1992). Annulus 1 is two kiloparsec wide and centered at 3.1 kpc, thus covering the current location of the inner ring. The centroids of annuli 2-9 are separated by 1.25 kpc, with the 2-nd annulus centered at 6.8 kpc. The 0-th annulus represents the nucleus. The mass of stars formed in each annulus is distributed into individual stellar masses using the Salpeter IMF with $\alpha = 1.35$ and the stellar mass interval of m_1=0.1 $M_\odot$ and m_2=100 $M_\odot$. The luminosity of each annulus at a given band A after time t can be computed as:

$$L_A(t) = \sum_m \sum_{\tau_m} l_A(m,\tau_m) N(m,\tau_m,t), \qquad (5)$$

where $N(m,\tau_m,t)$ is the number of stars in a given annulus at time t with mass m and age τ_m, and $l_A(m,\tau_m)$ is the luminosity of a star in the band A. Stellar luminosities $l_A(m,\tau_m)$ are obtained using stellar evolutionary (Schaller et al. 1992) and atmospheric (Kurucz 1992) models. The population synthesis code used in this work is explained in detail in Mayya (1995, 1997). This code synthesizes a number of observable quantities in the optical and near-infrared parts of the spectrum, which are suitable for comparison with the observed properties of giant star-forming complexes. Since the Cartwheel is a recent phenomenon with high rates of star formation, this code is especially suitable for our purposes. The results of this code are compared with those of other existing codes by Charlot (1996).

Classic Schmidt law of star formation ($n = 1.5$) is assumed throughout the paper (Kennicutt 1989). The half-width of a density enhancement L is chosen so as to reproduce the observed Hα surface brightness profile in the Cartwheel's outer ring (Higdon 1995). This gives the value of $L = 1$ kpc. Velocity of a propagating density enhancement $v = 55$ km s^{-1} is assumed to coincide with the expansion velocity of the outer ring $v = 53 \pm 9$ km s^{-1}, the value derived by Higdon (1996) from HI kinematics of the outer ring.

With the values of L and v being fixed, the coefficient a and the amplitude of density enhancement $A(r)$ constitute the set of parameters, which determine the number of stars $N(m,\tau_m,t)$ formed by a density wave in each photometric annulus (see eq. (5)). The birthrate of stars a relates the star formation rate observed in the Cartwheel galaxy with the assumed Schmidt law of star formation (see eq. (3)). We estimate its value for the Cartwheel's outer ring using the measured rate of star formation 67 $M_\odot$ yr^{-1} (Higdon 1995), the mean surface density of gas $\Sigma_{\rm gas} \approx 10\ M_\odot$ pc^{-2} (Higdon 1996) and the outer ring's area of 250 kpc^2. This gives the dimensionless value of $a = 0.0025$ when masses,

time scales, and distance scales are expressed in units $10^7\ M_\odot$, 10^6 yrs, and 1 kpc respectively.

We assume that the amplitude of density enhancement $A(r)$ is twice as big as the unperturbed, pre-collision gas surface density, which is typical for the spirals and is confirmed in numerical simulations by Appleton & Struck-Marcell (1987). To constrain the pre-collision radial profile of gas, we fit the model R-band and Hα surface brightness profiles of stellar populations formed in the expanding density wave to the profiles observed in the Cartwheel. We do this by varying the radial profile of gas in the pre-collision galactic disk.

4. Model B-V/V-K radial color gradients and $Q_{\rm BVK}$ indices of the Cartwheel galaxy.

4.1. Density wave in a purely gaseous disk.

As mentioned in the introduction, Korchagin et al. (2001) found that the density wave propagating in *a purely gaseous disk of uniform metallicity* cannot reproduce the Cartwheel's $B-V/V-K$ radial color gradient. The model colors are much bluer as compared to those observed in the Cartwheel. Korchagin et al. (2001) argued that the pre-collision disk of old stars was needed to reconcile the model and the Cartwheel's colors. We mainly confirm their conclusion. However, use of the extinction-free $Q_{\rm BVK}$ indices allows us to notice some interesting features that have been missed by Korchagin et al. (2001).

As in Korchagin et al. (2001), we consider the expanding density wave in a purely gaseous disk with five different metallicities: $z_\odot/20$, $z_\odot/5$, $z_\odot/2.5$, $z_\odot$, and $2z_\odot$. Our computations show that the model $B-V$ and $V-K$ colors are bluer as compared to the Cartwheel's colors for each metallicity of the star-forming gas. If dust extinction were solely responsible for this difference between the model and observed colors, then the model $Q_{\rm BVK}$ indices would lie within the observed limits. Indeed, use of the $Q_{\rm BVK}$ indices minimises the uncertainties in observed colors introduced by dust extinction. However, we find that the model $Q_{\rm BVK}$ indices lie beyond the observed limits *for most of the photometric annuli*, thus indicating that the reddening of the observed colors with respect to the model colors *of those annuli* cannot be attributed to the extinction gradient in the Cartwheel's disk.

In case of $z_\odot/2.5$ and $z_\odot/5$, however, the $Q_{\rm BVK}$ indices of the Cartwheel's outer region (annuli VI-IX) lie within the observed limits, thus indicating that dust extinction could be responsible for the reddening of the observed colors in this region. Here, we note that Korchagin et al. (2001) used a uniform metallicity of $z_\odot/20$ to model the Cartwheel's radial color gradient. While this choice is certainly justified for the Cartwheel's outer ring (Fosbury & Hawarden 1977), it is hard to believe that such a low metallicity is present in the Cartwheel's central regions. Due to very weak line emission, there have been no measurements of heavy element abundances interior to the outer ring. However, it is known that most galactic disks have a metallicity gradient, with metallicities in the nucleus up to ~ 10 times higher than in the outer parts of the disk (Smartt & Rolleston 1997). In this paper we assume that metallicity gradient is present in the pre-collision gaseous disk of the Cartwheel galaxy and choose its value so as to provide a better fit of the model $Q_{\rm BVK}$ indices with those observed in the Cartwheel's disk. The best fit is found for the metallicity gradient spanning the range from $z = z_\odot/3.75$ at annuli IX, VIII, and VII, $z = z_\odot/2.5$ at annuli VI and V, to $z = z_\odot$ at annuli IV-nucleus.

The open circles in Fig. 4a show the model $B-V/V-K$ colors of stellar populations formed in the density wave propagating in a purely gaseous disk with the metallicity gradient given above. The open circles in Fig. 4b illustrate the corresponding model $Q_{\rm BVK}$ indices. The outer three photometric annuli (9, 8, and 7) and the nucleus are identified both for the model colors and the colors observed in the Cartwheel galaxy, the latter being shown by the filled triangles with error bars. The model $B-V/V-K$ colors do not exhibit a regular reddening towards the nucleus and are bluer as compared to the Cartwheel's colors. On the same time, the model and the Cartwheel's $Q_{\rm BVK}$ indices show a good correspondence for the outer ring and two inner annuli adjacent to the outer ring, implying that the difference of the corresponding $B-V/V-K$ colors in Fig. 4a might be related to the internal extinction gradient existing in the Cartwheel's disk.

Now we consider an extreme case and assume that the difference of the model and observed $B-V/V-K$ colors in Fig. 4a is solely due to internal extinction gradient in the Cartwheel's disk. We warn, however, that this assumption is applicable only to those annuli, which $Q_{\rm BVK}$ indices lie within the observed limits, as in this case their colors are reddened along the correction vector. The values of color excess $E(B-V)$, implied by this difference, are listed in Col. 2 of Table 1. The surface densities of gas $\Sigma^{\rm ext}_{\rm HI+H_2}$ in Col. 3 are obtained from Col. 2 using the standard mass-to-dust ratio and $R_{\rm V} = 3.1$ (Bohlin et al. 1978). Column 4 in Table 1 gives the observed surface densities of atomic and molecular hydrogen $\Sigma^{\rm obs}_{\rm HI+H_2}$ in each annulus (Higdon 1996, Horellou et al. 1998).

Table 1. Extinction-estimated and observed surface densities of HI and H_2 in the Cartwheel

annulus	$E(B-V)$ (mag)	$\Sigma^{\rm ext}_{\rm HI+H_2}$ $M_\odot$ pc^{-2}	$\Sigma^{\rm obs}_{\rm HI+H_2}$ $M_\odot$ pc^{-2}
VI	$0^m.13$	5.7	≤ 4.5
VII	$0^m.07$	3.1	≤ 4.5
VIII	$0^m.14$	6.1	9.3-16
IX	$0^m.25$	10.9	9.3-16

It can be noticed that the extinction-estimated gas densities in Col. 3 are below the detection upper limit for the outer ring+annulus VII. Hence, the internal extinction gradient can indeed be responsible for the difference

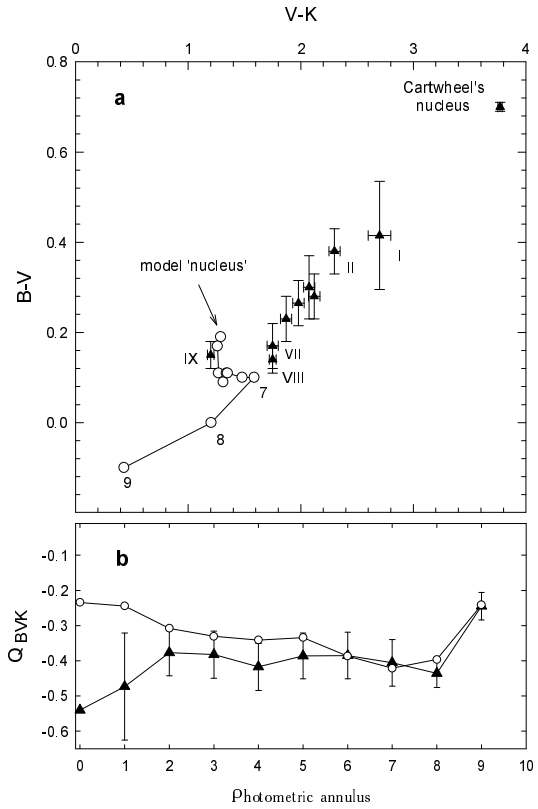

Fig. 4. (**a**) The $B-V$ and $V-K$ color-color diagram and (**b**) the $Q_{\rm BVK}$ combined index profiles. The open circles show the model profiles for the density wave of amplitude $A(r) = 70\exp(-r/12) M_{\odot}{\rm pc}^{-2}$ and velocity $v = 55{\rm kms}^{-1}$ expanding radially in a purely gaseous disk. The metallicity gradient of the gaseous disk ranges from $z = z_{\odot}$ at the nucleus+annuli I-IV, $z = z_{\odot}/2.5$ at annuli V-VI, to $z = z_{\odot}/3.75$ at annuli VII-IX. The filled triangles with error bars show the radial color gradients and index profiles observed in the Cartwheel galaxy.

between the observed and model $B-V/V-K$ colors of this region in Fig. 4a.

Very large values of Hα equivalent widths were found by Higdon (1995) in the Cartwheel's outer ring, especially in the ring's southern quadrant, which peaks at $EW_{\rm H\alpha} = 1250$ Å and exceeds 400 Å everywhere. The Hα equivalent width ($EW_{\rm H\alpha}$) is sensitive to the ratio of ionizing, massive ($> 10\ M_{\odot}$) stars to lower mass red giant stars and can be used to measure the relative strengths of these two populations (Kennicutt 1983). Table 2 presents $EW_{\rm H\alpha}$ of stellar populations born in the expanding ring density wave. $EW_{\rm H\alpha}$ are computed at the time when the wave reaches the present position of the Cartwheel's outer ring at 16 kpc. All parameters of Fig. 4 are retained. As it is seen in Table 2, the averaged over annuli VIII and IX model value of 335 Å is close to the azimuthally averaged value of 360 Å measured in the Cartwheel's outer ring by Higdon (1995). The large model and observed $EW_{\rm H\alpha}$ in the outer ring indicate that the Cartwheel is experiencing the first major episode of star formation *at this radius*.

Table 2. Model Hα equivalent widths

annulus	VI	VII	VIII	IX
$EW_{\rm H\alpha}$ (Å)	0.03	0.3	53	620

Korchagin et al. (2001) argued that the colors of the Cartwheel galaxy cannot be reproduced by a density wave propagating in a purely gaseous disk irrespective of its metallicity. While this is certainly true for the Cartwheel's inner region, we find that the observed $B-V/V-K$ colors and $Q_{\rm BVK}$ indices of *the outer ring+annulus VII* can be well reproduced by a density wave propagating in a purely gaseous disk of $z = z_{\odot}/3.75$.

4.2. The pre-collision old stellar disk.

To reconcile the model and observed $B-V/V-K$ colors and $Q_{\rm BVK}$ indices of the Cartwheel's inner region in Fig. 4 (annuli VI-nucleus), we follow the prescriptions given in Korchagin et al. (2001) and consider a possibility that the pre-collision Cartwheel had an old stellar disk. We assume that the properties of the old stellar disk are typical for the late-type Freeman disks ($\mu_V^0 = 21.0$ mag arcsec^{-2} and $R_0 = 2$ kpc) rather than for low surface brightness galaxies ($\mu_V^0 = 23.5$ mag arcsec^{-2} and $R_0 = 5$ kpc) as adopted by Korchagin et al. (2001). Metallicity of the pre-collision gaseous disk is assumed to span the range from $z = z_{\odot}/5$ at six outermost annuli to $z = z_{\odot}$ at the inner annuli and the nucleus. Galactic collision generates an expanding density wave, which adds the newly born stellar populations to the old stellar populations existed before the collision.

Figures 5a and 5b show the resulting model Hα and R-band surface brightness profiles. Interior to the outer ring, the model R-band profile shows a good correspondence to the observed profile, as illustrated in Fig. 5b by the open circles and filled triangles respectively. Measured by Higdon (1995) R-band surface brightness of the inner ring is roughly twice the peak value of the outer ring and this feature is well reproduced in Fig. 5b.

Table 3. Extinction-estimated and observed surface densities of HI and H_2 in the Cartwheel

annulus	$E(B-V)$ (mag)	$\Sigma^{\rm ext}_{\rm HI+H_2}$ $M_{\odot}$ pc^{-2}	$\Sigma^{\rm obs}_{\rm HI+H_2}$ $M_{\odot}$ pc^{-2}
II	$0^m.07$	3.1	≤ 4.5
III	$0^m.07$	3.1	≤ 4.5
IV	$0^m.07$	3.1	≤ 4.5
V	$0^m.07$	3.1	≤ 4.5
VI	$0^m.07$	3.1	≤ 4.5
VII	$0^m.06$	2.6	≤ 4.5
VIII	$0^m.15$	6.6	9.3-16
IX	$0^m.26$	11.4	9.3-16

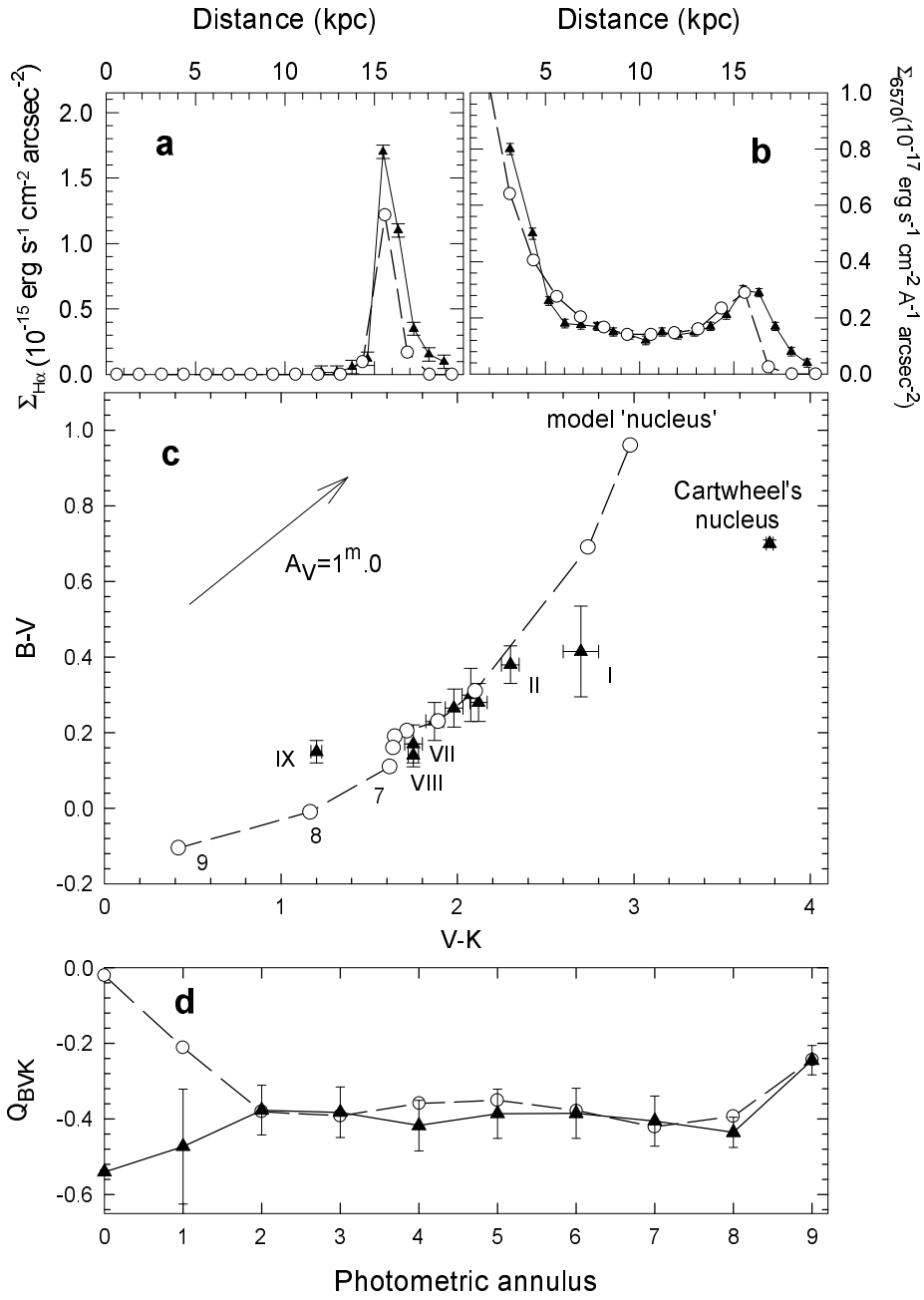

Fig. 5. The radial surface brightness profiles in (**a**) Hα and (**b**) R-band, (**c**) the $B-V/V-K$ color-color diagram, and (**d**) the $Q_{\rm BVK}$ radial profiles. The open circles show the model profiles for the density wave of amplitude $A(r) = 50\ \exp(-r/15)\ M_\odot\ {\rm pc}^{-2}$ and velocity $v = 55\ {\rm km\ s}^{-1}$ expanding radially in the galactic disk. The central surface brightness in the V-band of the old stellar component of the galactic disk is $\mu_{\rm V}^0 = 21.0$ mag arcsec^{-2} and the scale length is $R_0 = 2$ kpc. The gaseous component has the metallicity gradient ranging from $z = z_\odot$ at the nucleus+annuli I-III to $z = z_\odot/5$ at annuli IV-IX. The filled triangles with error bars show (**a,b**) the measured radial surface brightness profiles, (**c**) the radial color gradients and (**d**) index profiles of the Cartwheel galaxy.

The model radial $B-V/V-K$ colors, shown by the open circles in Fig. 5c, exhibit regular reddening towards the nucleus reminiscent of that observed in the Cartwheel's disk. The sequence of $Q_{\rm BVK}$ indices observed in the Cartwheel's outer ring and the inter-ring region is well reproduced, as shown by the open circles in Fig. 5d. This implies that the difference of the model and observed colors for each photometric annulus can be understood in terms of internal extinction. This is certainly not true for the Cartwheel's inner ring and the nucleus, as their

$B-V/V-K$ colors are not reddened along the correction vector with respect to the model colors. This results in a substantial disagreement of the corresponding $Q_{\rm BVK}$ indices. As in Sect. 4.1, we consider an extreme case and assume that the difference of the model and observed $B-V/V-K$ colors of the outer ring and the inter-ring region in Fig. 5c is solely due to internal extinction gradient in the Cartwheel's disk. The values of $E(B-V)$ implied by this difference are listed in Col. 2 of Table 3.

It can be noticed that the extinction-estimated gas densities in Col. 3 are below the detection upper limit in Col. 4 for all annuli. Hence, the internal extinction gradient can be responsible for the difference between the observed and model $B-V/V-K$ colors of the inter-ring region and the outer ring in Fig. 5c.

Comparison of Figs. 4a and 5c shows that the model $B-V/V-K$ colors of the outer ring+annulus VII in Fig. 5c are not affected noticeably by the old stellar populations. Indeed, Fig. 6 illustrates the ratio of fluxes of the old stellar populations to the young density-wave-born stellar populations in V-band ($F_{\rm V}[o/dw]$) and K-band ($F_{\rm K}[o/dw]$) as a function of galactic radius. It is seen that the old stellar populations dominate at the smaller radii ($R \leq 3$ kpc) in both bands. At the intermediate radii ($3 < R \leq 12$ kpc), input from the young stellar populations to the total flux in V-band is ten times (on average) the input from the old stellar populations, while both stellar populations contribute comparable fluxes in K-band. The young stellar populations totally dominate at the larger radii ($R > 12$ kpc) in both bands. This indicates that the colors of the Cartwheel's outer ring *are determined by the young density-wave-born stellar populations* and can be reproduced by a density wave propagating in a purely gaseous disk, as argued in Sect. 4.1. We note, however, that the interpretation of colors of the Cartwheel's inner region do require the presence of the old pre-collision stellar disk, which is in agreement with conclusions of Korchagin et al. (2001).

Thus, theoretical modelling of the color gradients observed in the Cartwheel galaxy suggests that the pre-collision Cartwheel was a late-type spiral ($R < 12$ kpc) embedded into an extensive HI disk. The subcritical gas disk of $\Sigma_{\rm HI} \leq 11\ M_\odot$ pc^{-2} (Higdon 1996) at larger radii ($R \geq 12$ kpc) prevented robust massive star formation (MSF) and chemical enrichment over the disk's lifetime. The passage of a companion galaxy initiated an outwardly propagating ring density wave, which triggered high rates of MSF along it's perimeter. The density wave has passed the original extend of the pre-collision stellar disk and is currently moving in the predominantly gaseous, low-metallicity disk at the radius of the Cartwheel's outer ring ($R \approx 16$ kpc).

Another result of color modelling is a possible presence of a large internal extinction gradient across the outer ring of the Cartwheel (annuli VIII and IX). Indeed, if the difference between the model and observed $B-V/V-K$ colors of the Cartwheel's outer ring in Figs. 4a and 5c can be attributed to the internal extinction as shown above,

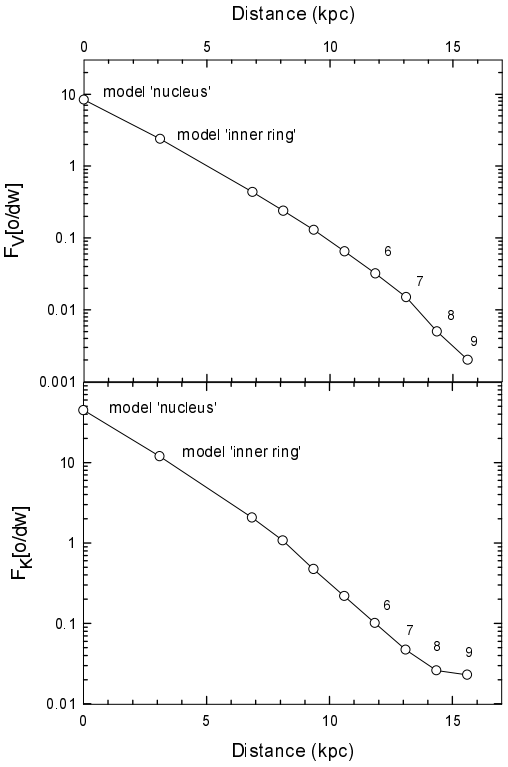

Fig. 6. The ratio of fluxes in V-band (the upper frame) and K-band (the lower frame) of the old, pre-collision stellar populations to the young stellar populations formed in the density wave. All parameters of Fig. 5 are retained. The numbering of annuli is in accordance with Fig. 1.

then $E(B-V)$ in the outer edge of the outer ring (annulus IX) is about two times higher as compared to $E(B-V)$ in the inner edge of the outer ring (annulus VIII). Models of ring galaxies predict that the Cartwheel's outer ring is the current location of a star formation wave (Appleton & Struck-Marcell 1987, Struck-Marcell & Appleton 1987). The star formation wave is expected to compress the gas ahead by a coherent action of shock waves, expanding superbubbles, ultraviolet radiation from massive stars, ets., thus increasing the value of extinction at the leading edge of the wave. Observationally proved presence of such an extinction gradient across the outer ring might be a powerful confirmation of propagating nature of star formation in ring galaxies. More sophisticated models of star formation in the ring galaxies are needed to investigate these aspects.

5. The inner ring and the nucleus

In the cloud-fluid models of ring galaxies, Appleton & Struck-Marcell (1987) predicted that the infall of gas behind the ring should lead to a strong compression of gas in the central parts. In case of the Cartwheel galaxy, a large-

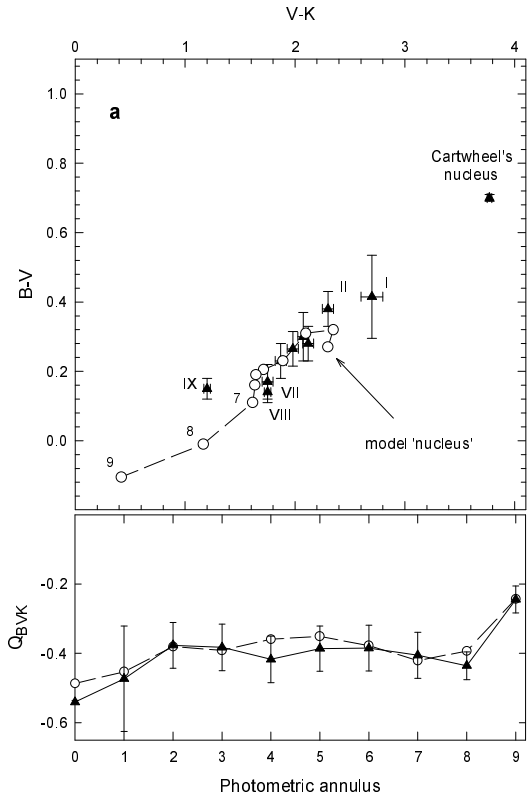

Fig. 7. (**a**) The $B-V/V-K$ color-color diagram, and (**b**) the $Q_{\rm BVK}$ radial profiles. All parameters are the same as in Fig. 5, but with an additional 10-Myr-old burst of star formation in the Cartwheel's nuclear region.

scale radial infall of HI was reported by Higdon (1996). Recent observation in the mid-infrared (Charmandaris et al. 1999) and in Hα line (Amram et al. 1998) have shown that the Cartwheel's inner ring and the nucleus might have a low level star formation activity.

In this section, we perform numerical modelling of the $B-V/V-K$ colors and $Q_{\rm BVK}$ indices measured in the Cartwheel's inner ring and the nucleus (Marcum et al. 1992). To do this, we assume that the star formation takes place not only along the perimeter of the expanding density wave, but also in the central region of the Cartwheel. We set off an outwardly propagating density enhancement of amplitude $A(r) = 50\ \exp(-r/15)\ M_\odot\ {\rm pc}^{-2}$ and velocity $v = 55$ km s^{-1} and compute the luminosity of pre-collision and post-collision stars as in Sect. 4. Then we add the luminosity of stars born in the central region and use the total luminosity in each annulus to calculate the resulting surface brightness, color, and index profiles.

While the inner ring and the nucleus are currently HI poor with $\Sigma_{\rm HI} \leq 0.3\ M_\odot\ {\rm pc}^{-2}$ (Higdon 1996), they have a significant amount of molecular hydrogen as suggested by recent CO observations of Horellou et al. (1998). We assume that molecular hydrogen in the Cartwheel is exponentially distributed in the central 9.5 kpc, with the peak surface density of 35 $M_\odot\ {\rm pc}^{-2}$ in the nucleus and the scale length of 3 kpc (radius of the inner ring). The total mass of H_2 is then close $1.6\times10^9\ M_\odot$, as estimated by Horrelou et al. (1998) for the solar metallicity. Metallicity in the central part of the Cartwheel is unknown. We assume that star-forming gas in the central 9.5 kpc is of solar metallicity, as suggested by numerical modelling in Sect. 4. The star formation law in the nucleus and the inner ring is assumed to follow the classic Schmidt behavior:

$$SFR = a\ \Sigma_{\rm H_2}^{1.5}, \qquad (6)$$

with the rate of star formation a defined as in Eq. (3).

We use two conventional models for star formation: a constant star formation and a short starburst. In both models star formation proceeds until $1.6\times10^8\ M_\odot$ of stars is formed, which is 10% of the initial mass of gas. In the short starburst model we increase the rate of star formation a to shorten the star formation event.

Constant star formation in the nuclear region for the last 60 Myr. Assumption of the constant star formation activity in the Cartwheel's central region allows us to reach a better agreement between the model and observed $B-V/V-K$ colors and $Q_{\rm BVK}$ indices of the nucleus and the inner ring. The model $Q_{\rm BVK}$ index of the inner ring lies within the observed limits, which is not the case in Fig. 5d. Now, however, the inner ring+nucleus and the outer ring have comparable Hα fluxes. This is problematic since observations indicate that the Cartwheel lacks strong Hα emission from the nucleus and the inner ring, while it has a large Hα luminosity in the outer ring (Higdon 1995, Amram et al. 1998). We assume that the lack of strong Hα emission from the nucleus and the inner ring is the result of a burst-like nature of star formation in the nuclear region. If the active star formation in the nucleus+inner ring had ceased about ten million years ago, then the observed Hα flux would have fallen considerably at present.

Short starburst in the nuclear region. Infall of gas into central parts of a galaxy is known to trigger starbursts. We assume that the large-scale radial infall of gas, reported by Higdon (1996), has triggered a short starburst in the Cartwheel's nucleus and the inner ring ten million years ago. The resulting model $B-V/V-K$ radial color gradients and $Q_{\rm BVK}$ radial profiles are illustrated with the open circles in Figs. 7a and 7b respectively, while the filled triangles with error bars indicate the corresponding radial profiles observed in the Cartwheel galaxy. The sequence of $Q_{\rm BVK}$ indices observed in the galaxy is well reproduced, as shown by the open circles in Fig. 7b. Now, the model peak value of Hα surface brightness at the outer ring is 60 times larger than the model peak value at the nucleus, which is close to what is observed in the Cartwheel galaxy (Amram et al. 1998).

The difference of the model and Cartwheel's $B-V/V-K$ colors of the inner ring (annulus I) and the nucleus, which is seen in Fig. 7a, can be explained in terms of internal extinction using the same approach as in Sect. 4. Implied by this difference, color excess $E(B-V)$ of the Cartwheel's nucleus is $0^{\rm m}.43$, which is equivalent to

$\Sigma_{\rm HI+H_2}$ of 19 $M_\odot$ pc^{-2} (Bohlin et al. 1978). If molecular hydrogen is exponentially distributed in the central 9.5 kpc, then this value of $\Sigma_{\rm HI+H_2}$ might be below the detection upper limits of molecular hydrogen in the Cartwheel's nucleus. Hence, the internal extinction can be responsible for the difference between the model and observed $B-V/V-K$ colors of the nucleus shown in Fig. 7a. This conclusion is also true for the Cartwheel's inner ring, where $\Sigma_{\rm HI+H_2} = 4.5\ M_\odot$ pc^{-2} is inferred using $E(B-V) = 0^{\rm m}.1$. Now, the young post-collision stellar populations and the old pre-collision stellar populations contribute equally to the total flux in the V- and K-bands at the smaller radii ($R \leq 3\ kpc$).

6. Conclusions

In this paper we model and analyse the $B-V/V-K$ radial color gradients observed in the Cartwheel ring galaxy. We use the $Q_{\rm BVK}$ combined color indices to analyse the Cartwheel's $B-V/V-K$ radial color gradients. Use of the $Q_{\rm BVK}$ indices minimises the uncertainties in the observed $B-V$ and $V-K$ colors introduced by dust extinction. We find that the $Q_{\rm BVK}$ radial profile observed in the Cartwheel's disk falls naturally into three sub-profiles, which correspond to the nucleus+inner ring, the inter-ring region, and the outer ring of the galaxy. Combined color indices are insensitive to dust extinction and can be directly understood in terms of stellar populations. This implies that the nucleus+inner ring, inter-ring region, and the outer ring of the Cartwheel might consist of different stellar populations.

To model the optical and near-infrared color properties of the Cartwheel galaxy, we use a toy model, which imitates the propagating star formation in the galactic disk. Namely, we assume that the star formation rate is proportional to a Gaussian density enhancement, expanding radially in a gaseous disk. We use the population synthesis to calculate the color properties of stellar populations formed by this density enhancement.

The results of color modelling strongly suggest that the pre-collision Cartwheel was a late-type spiral. The old stellar disk was embedded in an extensive gaseous disk of sub-critical surface density. Existence of the pre-collision stellar disk of low surface brightness $\mu_V^0 = 23.5$ mag arcsec^{-2}, extending out to the current location of the Cartwheel's outer ring at 16 kpc ($R_0 = 5$ kpc), was first reported by Korchagin et al. (2001). However, we find that the pre-collision stellar disk might be smaller, extending out to ≈ 12 kpc. Properties of the pre-collision stellar disk are typical for the late-type Freeman disks ($\mu_V^0 = 21.0$ mag arcsec^{-2} and $R_0 = 2$ kpc) rather than for low surface brightness galaxies as found by Korchagin et al. (2001). The pre-collision gaseous disk had a metallicity gradient ranging from $z = z_\odot/5$ at the outer parts to $z = z_\odot$ in the central parts. Approximately 300 Myr ago, the Cartwheel galaxy collided face-on and near-centrally with a companion galaxy. This collision generated an expanding ring density wave, which triggered massive star formation along the wave's perimeter.

The results of our modelling show that the young stellar populations, formed by the density wave, dominate in the outer ring. Thus, the wave of star formation has passed the extent of the pre-collision stellar disk and is currently moving in the predominantly gaseous, low-metallicity disk at the radius of 16 kpc. In the region between the inner and the outer rings, however, the young stellar populations and the pre-collision stellar populations contribute comparable fluxes in K-band. We find that the Cartwheel's $B-V/V-K$ colors and $Q_{\rm BVK}$ indices of this inter-ring region cannot be successfully modelled without taking into consideration the relative input from the old, pre-collision stellar populations.

The observed colors of the nucleus+inner ring are most difficult to model. Neither young stellar populations formed in the expanding density wave, nor their mixture with the old, pre-collision stellar populations can reproduce the $B-V$ and $V-K$ colors of the Cartwheel's nucleus+inner ring. We find that an additional 10-Myr-ago burst of star formation in the nuclear regions, along with the visual extinction of $A_V = 1^{\rm m}.3$, might be responsible for the peculiar colors of the Cartwheel's nucleus. This is not totally unexpected, as some observational evidence points to the existence of a low-level star formation activity in the central regions (Amram et al. 1998, Charmandaris et al. 1999) and the large-scale radial infall of gas in the Cartwheel, reported by Higdon (1996), might have triggered bursts of star formation in the past.

Acknowledgements. The authors thank two anonymous referees for useful comments. The authors are grateful to Dr. Y.D. Mayya for providing his population synthesis program. Our special thanks are to Dr. V. Korchagin for continuous encouragement. We also thank Dr. de Jong for providing his observational data.

References

Amram, O., Mendes de Oliveira, C., Boulesteix, J., & Balkowaki, C. 1998, A&A, 330, 881
Appleton, P.N., & Marston, A.P. 1997, AJ, 113, 201
Appleton, P.N., & Struck-Marcell, C. 1987, ApJ, 318, 103
Bica, E., & Alloin, D. 1987, A&A, 186, 49
Bizyaev D., Zasov A., & Kajsin S. Proc. of 33rd ESLAB Symp. "Star formation from the small to the large scale", (Eds. F.Favata, A.A. Kaas & A. Wilson, ESA SP-445, 2000)
Bizyaev D., Zasov A., & Kaisin S. 2001, Astronomy Letters, 27, 217.
Bohlin, R.C., Savage, B.D., & Drake, J.F. 1978, ApJ, 224, 225
Cardelli, J.A., Geoffrey, C.C., & Mathis, J.S. 1989, ApJ, 345, 245
Charlot, S. 1996, in ASP Conf. Ser. 98, From Stars to Galaxies, Ed. C. Leitherer, U. Fritze-v. Alvensleben, & J. Huchra (San Francisco: ASP), 275
Charlot, S., & Bruzual, A. 1991, ApJ, 367, 126
Charmandaris, V., Laurent, O., Mirabel, et al. 1999, A&A, 341, 69
de Jong, R.S., 1996, A&A, 313, 377

Fosbury, R.A.E., & Hawarden, T.G. 1977, MNRAS, 178, 473
Freeman, K.C. 1970, ApJ, 160, 811
Higdon, J.L. 1995, ApJ, 455, 524
Higdon, J.L. 1996, ApJ, 467, 241
Horellou, G., Charmandaris, V., Combes, et al. 1998, A & A, 340, L51
Kennicutt, R.C. 1983, ApJ, 272, 54
Kennicutt, R.C. 1989, ApJ, 344, 685
Korchagin, V., Mayya, Y.D., & Vorobyov, E.I. 2001, ApJ, 554, 281
Kurucz, R.L. 1992, IAU Symp. 149, Stellar Populations of Galaxies, Ed. B. Barbuy & A. Renzini (New York: Kluwer), 225
Marcum, P.M., Appleton, P.N., & Higdon, J.L. 1992 ApJ, 399, 57
Mayya, Y.D. 1995, AJ, 109, 2503
Mayya, Y.D. 1997, ApJL, 482, L149
Schaller, G., Schaerer, D., Meynet, G., & Maeder, A. 1992, A&AS, 96, 269
Smartt, S.L., & Rolleston, W.R.J. 1997, ApJ, 481, L47
Struck-Marcell, C., & Appleton, P.N. 1987, ApJ, 323, 480
Zasov, A.V., & Moiseev, A.V. 1998, Astronomy Letters, 24, 677
Worthey, G. 1994, ApJSS, 95, 107